Evaluation of the Tauc Method for Optical Absorption Edge Determination: ZnO Thin Films as a Model System

Viezbicke, Brian D.; Patel, Shane; Davis, Benjamin E.; et.al.

Viezbicke, B. D., Patel, S., Davis, B. E., & Birnie, D. (2015). Evaluation of the Tauc Method for Optical Absorption Edge Determination: ZnO Thin Films as a Model System (, Ill.). In Physica Status Solidi, B (Vol. 252, Issue 8, pp. 1700–1710). Wiley-VCH. https://doi.org/10.7282/T3W097T7

RUTGERS UNIVERSITY

Dept. of Materials Science and Engineering
McLaren Center for Ceramic Research, 129
Rutgers, The State University of New Jersey
607 Taylor Road
Piscataway, NJ 08854-8065

www.mse.rutgers.edu
dunbar.birnie@rutgers.edu

Phone: 848-445-5605
Fax: 732-445-5595

Evaluation of the Tauc Method for Optical Absorption Edge Determination: ZnO Thin Films as a Model System

by

Brian D. Viezbicke, Shane Patel, Benjamin E. Davis, and Dunbar P. Birnie, III[#]

Final bibliographic citation of published work: B. D. Viezbicke, Shane Patel, B. E. Davis and D. P. Birnie, III, "Evaluation of the Tauc Method for Optical Absorption Edge Determination: ZnO Thin Films as a Model System", Physica Status Solidi, B, **252**, 1700-1710 (2015), (DOI:10.1002/pssb.201552007).

Our paper was also featured as the back cover artwork for the August issue (in which our paper appeared): Here is a preview of that artwork.

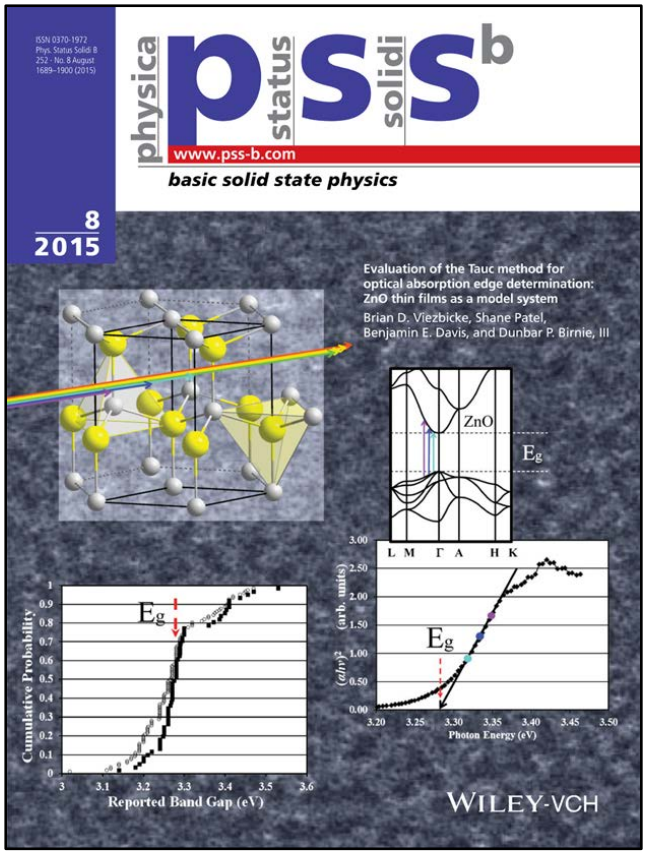

Abstract

One of the most frequently used methods for characterizing thin films is UV-Vis absorption. The near-edge region can be fitted to a simple expression in which the intercept gives the band-gap and the fitting exponent identifies the electronic transition as direct or indirect. (See Tauc et al., Physica Status Solidi, 1966; these are often called "Tauc" plots.) While the technique is powerful and simple, the accuracy of the fitted band-gap result is seldom stated or known. We tackle this question by refitting a large number of Tauc plots from the literature and look for trends. Nominally pure zinc oxide (ZnO) was chosen as a material with limited intrinsic deviation from stoichiometry and which has been widely studied. Our examination of the band gap values and their distribution leads to a discussion of some experimental factors that can bias the data and lead to either smaller or larger apparent values than would be expected. Finally, an easily evaluated figure-of-merit is defined that may help guide more accurate Tauc fitting. For samples with relatively sharper Tauc plot shapes, the population yields Eg (ZnO) as 3.276 +/- 0.033 eV, in good agreement with data for single crystalline material.

[#] e-mail address: "dunbar.birnie@rutgers.edu"

Evaluation of the Tauc Method for Optical Absorption Edge Determination: ZnO Thin Films as a Model System

Brian D. Viezbicke, Shane Patel, Benjamin E. Davis, and Dunbar P. Birnie, III[#]

Department of Materials Science and Engineering

Rutgers University

Piscataway, NJ 08854-8065

Version as submitted: *Physica Status Solidi, B, 2015*

Final full bibliographic journal citation as published:
Physica Status Solidi, B, **252**, 1700-1710 (2015), (DOI:10.1002/pssb.201552007).

Abstract

One of the most frequently used methods for characterizing thin films is UV-Vis absorption. The near-edge region can be fitted to a simple expression in which the intercept gives the band-gap and the fitting exponent identifies the electronic transition as direct or indirect. (See Tauc et al., Physica Status Solidi, 1966; these are often called "Tauc" plots.) While the technique is powerful and simple, the accuracy of the fitted band-gap result is seldom stated or known. We tackle this question by refitting a large number of Tauc plots from the literature and look for trends. Nominally pure zinc oxide (ZnO) was chosen as a material with limited intrinsic

[#] e-mail address: "dunbar.birnie@rutgers.edu"

deviation from stoichiometry and which has been widely studied. Our examination of the band gap values and their distribution leads to a discussion of some experimental factors that can bias the data and lead to either smaller or larger apparent values than would be expected. Finally, an easily evaluated figure-of-merit is defined that may help guide more accurate Tauc fitting. For samples with relatively sharper Tauc plot shapes, the population yields Eg (ZnO) as 3.276 +/- 0.033 eV, in good agreement with data for single crystalline material.

Introduction

This paper describes an in-depth analysis of the Tauc method of optical absorption edge determination as applied specifically to direct band-gap materials. The Tauc method uses simple multi-wavelength absorption spectroscopy and is relied upon for materials evaluation of functional photovoltaic layers, transparent conductors, sensor coatings, and films used for many other applications. The seminal work by Tauc, Grigorovici, and Vancu [1] presented a simple and useful method for assessing amorphous thin-film materials, though the method is now broadly applied to crystalline thin films as well. While extensively used to explore phase development, there remains some question about its application to polycrystalline thin films as well as on the accuracy of the method. Our assessment of the Tauc method is performed on a material of simple stoichiometry known to form easily from many chemical routes: ZnO. A review of thin-film zinc oxide (ZnO) literature yielded a large set of papers that cited Tauc's seminal work and included plots of data measured on undoped samples. This body of work included over 120 individual Tauc plots that were used as the test population for the present study. Published plots were redigitized and a consistent methodology was applied to extract the

band gap per the Tauc method, as described in detail below. The band gap data were compared with their original source, yielding a determination of the basic precision of the method. Other aspects of the shape of Tauc plots are discussed as possible contributors to error in the method. Additionally we suggest a new figure of merit that helps identify plots with better inherent accuracy.

Zinc oxide is a good candidate for evaluating the Tauc method because it has been widely studied for a number of useful applications [2-20]. Among these applications the band-gap plays a central and fundamental role as it controls many absorption and conductivity phenomena. Single crystal optical studies have found a direct band gap of 3.3 eV[21-23], though many of the papers surveyed in the present thin film analysis have collected data from very well crystallized films or even epitaxially grown layers.

Numerous deposition methods are available for zinc oxide thin films including sol-gel[24-29], chemical vapor deposition [9, 18, 30, 31], hydrothermal [32, 33] or solvothermal growth[34], magnetron sputtering[35-38] and pulsed laser deposition (PLD)[39-42]. It is stable in a hexagonal wurtzite structure with lattice parameters of (c=5.205 A, a=3.249 A)[43]. While every stoichiometric compound must thermodynamically have point defects at *some* level (and therefore by definition be *non*-stoichiometric), the phase of ZnO has been experimentally studied and found to have very little deviation from the ideal 1:1 ratio. For example, the early work of Allsopp and Roberts found a slight zinc excess, but less than 50 ppm [44]. This is much more stoichiometric than many phases and thus provides a good calibration test-case for the Tauc method, as described further below.

Background

While investigating the optical and electronic properties of amorphous germanium, Tauc et al, proposed and substantiated a method for determining the band gap using optical absorbance data plotted appropriately with respect to energy [1]. This was further developed in Davis and Mott's more general work on amorphous semiconductors[45, 46]. They show that the optical absorption strength depends on the difference between the photon energy and the band gap as shown in (Eq. 1):

$$(\alpha h\nu)^{1/n} = A(h\nu - E_g) \qquad (1)$$

where h is Planck's constant, ν is the photon's frequency, α is the absorption coefficient, E_g is the band gap and A is a proportionality constant. The value of the exponent denotes the nature of the electronic transition, whether allowed or forbidden and whether direct or indirect:

For direct allowed transitions	n=1/2
For direct forbidden transitions	n=3/2
For indirect allowed transitions	n=2
For indirect forbidden transitions	n=3

Typically, the allowed transitions dominate the basic absorption processes, giving either n=1/2 or n=2, for direct and indirect transitions, respectively.

Thus, the basic procedure for a Tauc analysis is to acquire optical absorbance data for the sample in question that spans a range of energies from below the band gap transition to above it.

Plotting the $(\alpha h \nu)^{1/n}$ versus $(h \nu)$ is a matter of testing n=1/2 or n=2 to compare which provides the better fit and thus identifies the correct transition type.

Figure 1 gives one example Tauc plot for ZnO where the absorption coefficient times the photon energy to the second power is plotted versus the incident photon energy[47]. The second power was used as zinc oxide is well known to have a direct allowed transition. The characteristic features of Tauc plots are evident: at low photon energies the absorption approaches zero – the material is transparent; near the band gap value the absorption gets stronger and shows a region of linearity in this squared-exponent plot[1]. This linear region has been used to extrapolate to the X-axis intercept to find the band gap value (here about 3.27 eV). At even higher energies the absorption processes saturate and the curve again deviates from linear.

To select and justify a linear region for extrapolation one must understand the reasons for these lower and upper deviations from linear behavior. On the low energy end, the deviation from linearity can be associated with defect absorption states that are near the band edge. This phenomenon has been investigated by Urbach [48] and in subsequent years, therefore, identified as an "Urbach Tail." These states are usually described by an exponential function, corresponding to a typical distribution of density of states, evident in the absorption behavior seen in the example Tauc plot (Figure 1). On the high energy end, saturation of available transition states is responsible for a leveling out of absorption strength in most collected spectra.

[1] The region of linearity may seem rather narrow on an absolute energy basis (being only ~0.1 or ~0.2 eV wide in many cases). However, this is to be expected for direct band-gap materials, which are typically found to have extremely rapid rise in absorption coefficient value immediately above the band-gap energy – which is the basis for establishment of the Tauc method to begin with.

The next section explains more specifically how we have done the Tauc fitting of the data on ZnO presented by many authors previously.

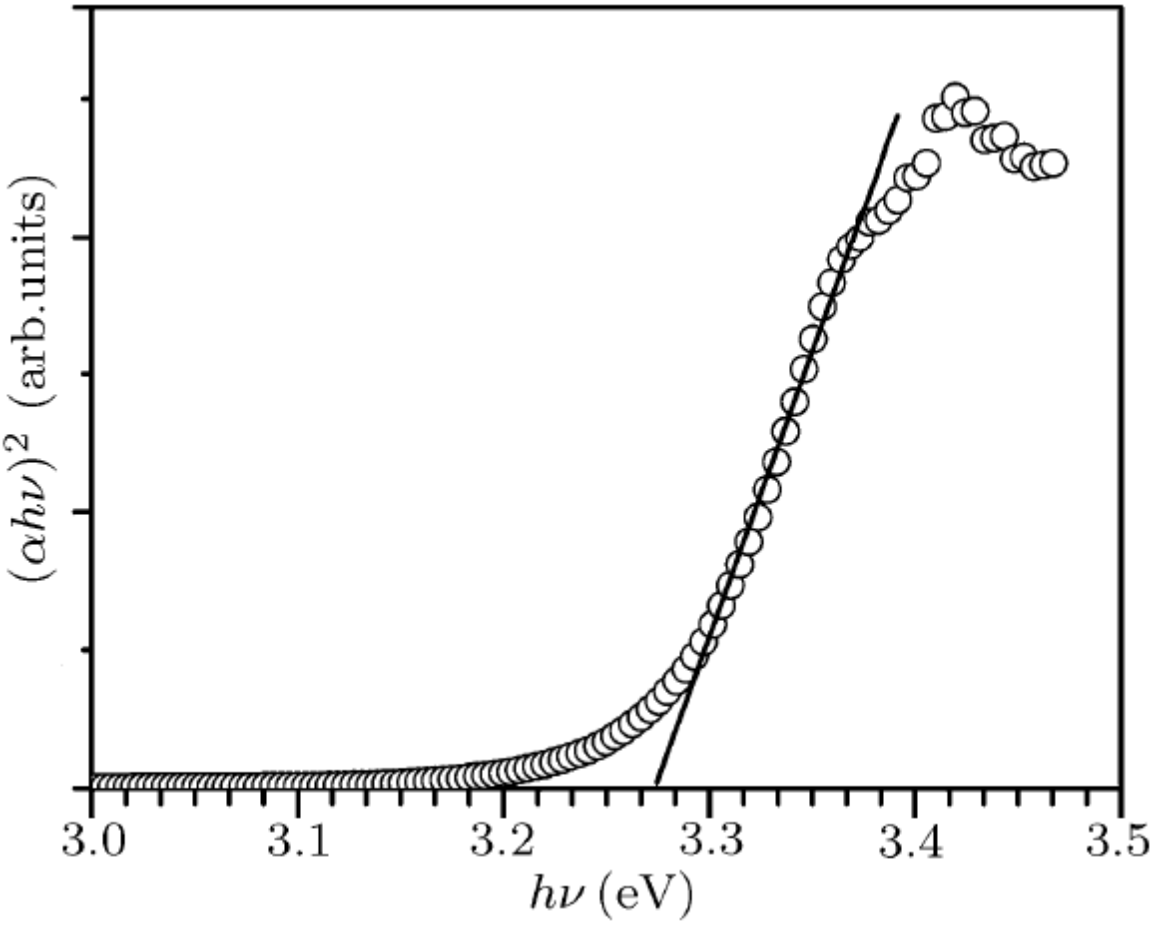

Figure 1: Example Tauc Plot from UV-Vis analysis of a ZnO thin film that illustrates the method of fitting the linear region to evaluate the band-gap at the X-axis intercept, here about 3.27 eV. Reprinted by permission from ref. [47].

Model

As noted above, we collected a large number of published Tauc analyses of undoped ZnO that included plots of the absorbance data against the photon energy [9, 26, 32-34, 36, 37, 49-119]. This was critical, as our assessment of the application of the Tauc method required the consistent application of a fitting method, as described below. Through the following method over 120 individual Tauc plots were re-assessed[2] to extract band gaps for comparison with the originally published results and to build a histogram of band gap values determined for this material. This population contained materials made with many deposition methods and varying process conditions with each method. Our digitization of the published plots was done using "Plot Digitizer"[3], to acquire data from digital (PDF) images of the graphs in each of the journal articles in question.

Each literature Tauc plot was digitized in the following manner: A screen captured digital image of the plot was collected at the highest resolution possible. The saved JPG image was imported into the digitizing software. Once imported, the process for digitization began with the assigning of origin, axes, and scale according to the published graphical data. Then each distinct data point was logged, or for smooth curves then reasonably closely spaced data points were digitized. Each "click" logged by the software was then saved in a data file specifying X (typically photon energy, eV) and Y (typically absorption Tauc function, $[(\alpha\, h\, \nu)^2]$) values.

[2] While this seems like a large number of Tauc analyses, we know that there are far more ZnO analyses in the literature that have also used the Tauc method, but may not have cited Tauc's original work directly. We believe that the present sample population is large enough to give an excellent representation of the larger body of ZnO works – and the Tauc method more specifically. These papers are not being endorsed nor are they being criticized; they are merely showing the range of variability of samples and band-gap determinations when studied by the Tauc method .

[3] (v. 2.6.2 - December 17, 2012 Build), written and freely distributed by Joseph A. Huwaldt and Scott Steinhorst

Each of the digitized data sets was first replotted and visually examined to ensure no artifacts of digitization were present as unrealistic outliers not corresponding to the originally published figures. Though there was no expected specific disagreement with the Tauc fitting presented by the source authors in any case, the present work tried to develop a completely unbiased method for picking the linear portion of the plot and finding the band gap value. The raw digitized data were then processed in a spreadsheet to achieve a series of linear regressions corresponding to incremental portions of each data set. We typically fitted using an 11-data-point window for evaluating the local linear regression (using +/- 5 datapoints on either side for any given local fit), and then we slid this fitting-window along and tested the fit at every possible location. The impact of fitting window width can be illustrated in Figure 2 where we plot the R^2 value for each incremental linear regression fit for the data we extracted from the graph shown in Figure 1. Three different curves are presented that cover 5, 11, and 15 datapoint windows, respectively. When fewer data points are used for fitting then better R^2 results are generally obtained (as a mathematical certainty). However, if the actual linear region is relatively short then using a bigger span of datapoints will force the inclusion of points that are clearly not part of the linear region and the R^2 value will be reduced. Or, similarly when fitting a line to a clearly curved part of the dataset, the same R^2 reduction will occur. Figure 2 illustrates this behavior with the general trend downward for the energy values between 3.2 and 3.3 eV (see arrow). Referring back to Figure 1, it can be seen that this is a region of upward curvature for the Tauc plot, so that extending the fit to larger ranges of data can force the inclusion of more curvature and therefore poorer fits (as shown). The best fit values are found in the mid-point photon energy region between 3.30 and 3.35 eV (as marked with the red ellipse in Figure 2), which corresponds to the energy range used by the original authors to fit the band gap, as shown by the line they

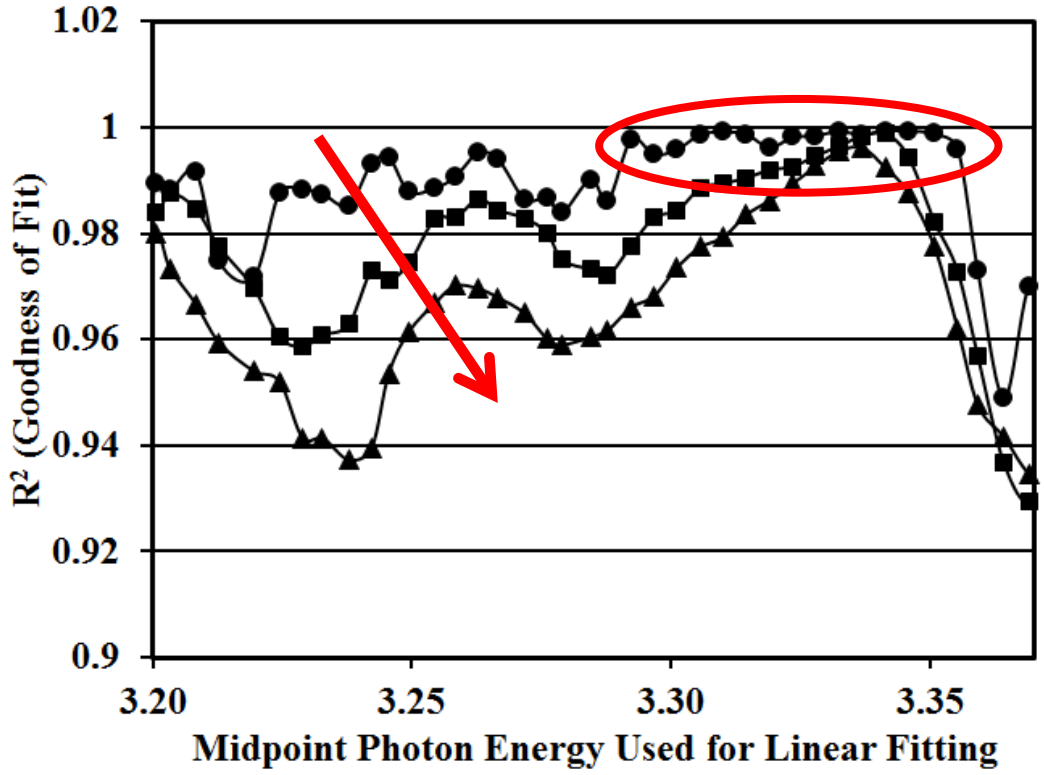

Figure 2: Linear regression fitting quality for different portions of the data as a method of choosing the best linear region for extrapolating the "Tauc gap": (●) 5 sequential data points, (■) 11 sequential points, and (▲) 15 sequential points used.

have drawn (see Figure 1). In our analysis, each linear regression can be evaluated to find the X-axis intercept (the band gap value). Figure 3 shows how this band gap/intercept value changes depending on which set of adjacent datapoints are used for linear regression fitting. The best R^2 values for fitting correspond to the band gap values highlighted with the ellipse, all around 3.28 eV. Note that the choice of the width of fitting window imposes only a slight change in extrapolated band gap value establishing a method-imposed precision of about +/-0.005 eV. Interestingly, the standard regression error from any specific fit can be used to calculate a

confidence interval for specific fit's extrapolated bandgap value. For the data shown in Figure 1-3 the best-fit region is found to have 95% confidence intervals of +/-0.0025 eV, +/-0.0015 eV, and +/-0.0023 eV, for the 5, 11, and 15 point fitting windows, respectively. The smaller fitting window has a better R^2 value, but the extrapolation is poorer because it is based on a narrower range of energy values and fewer data points. The largest fitting window has a wider basis for making the extrapolation, but the R^2 value is a little lower and the confidence interval a little wider, too. In any case, these confidence intervals must be considered the best precision values for the technique, though when many measurements are considered and compared the accuracy is not as good as this. It should be noted that at much lower energy values (below 3.2 eV for this

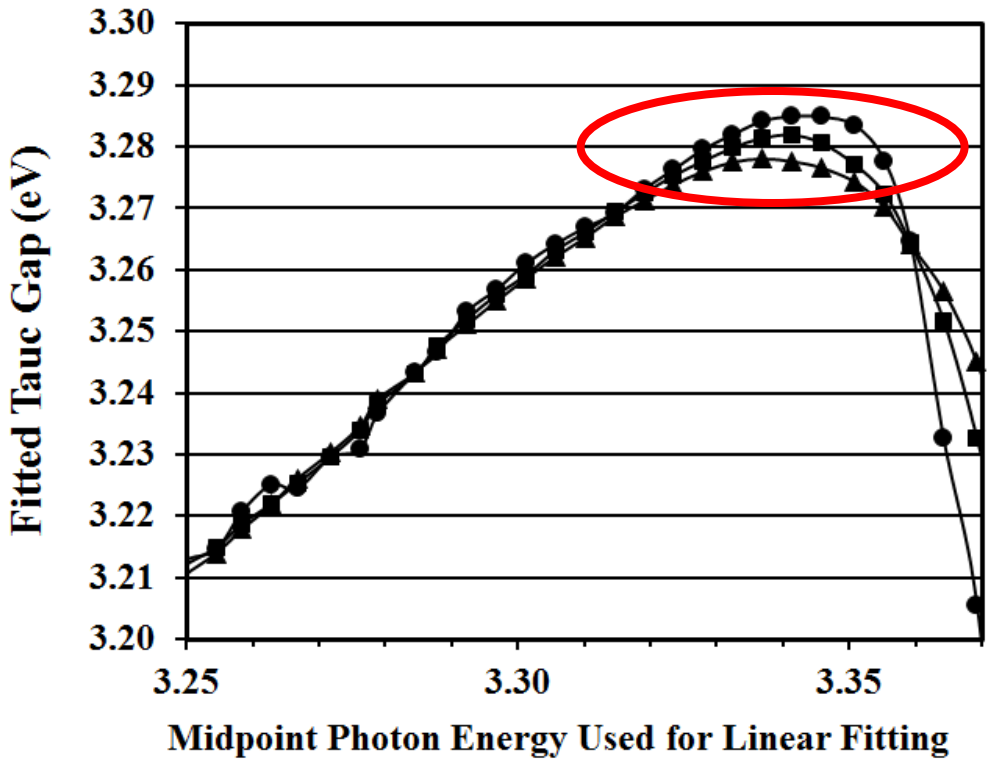

Figure 3: Fitted Tauc gap obtained from linear regression fits covered in Figure 2. The region where the best R-squared values were obtained is also the region where the fitting slope is steepest and the largest Tauc gap intercept is found: (●) 5 sequential data points, (■) 11 sequential points, and (▲) 15 sequential points used.

dataset) the extended range of the Urbach tail will also give good linear fits, but the preferred answers will typically correspond to the steepest region of the Tauc plot and yield the largest Tauc gap (intercept) values as emphasized by the shape of Figure 3.

In the case of amorphous silicon, which has a gradual absorption edge and more pronounced Urbach tail, the difficulty of finding the linear region to fit has been discussed by Sweenor et al.[120] based on earlier comments by Dawson et al.[121] that suggested errors as large as 0.3 eV in some cases. So, in summary, the present work has used the R^2 value itself to identify the section of the data that is most linear, and the line from this region is used to find the extrapolated Tauc gap. And, as shown in Figures 2 and 3, when some of the datapoints from the Urbach tail region happen to be included in the fit the tendency will be to yield Tauc gaps that are slightly lower than are found for less defective samples with more linear plot regions.

In view of the importance of the overlap between the linear region used for Tauc gap fitting and the lower energy Urbach tail absorption effects we also have tried to provide a quantitative measure for comparing different plots and data. We note that if there were no Urbach tail at all then the absorption would be zero up to the optical gap and then rise linearly according to equation (1). So we suggest that the $(\alpha h\nu)^2$ value measured at the Tauc gap should relate to the size of the Urbach tail, though perhaps not to its energy breadth or shape in detail. Often the Tauc plots are put on an arbitrary units scale, so we normalize this value by comparing it to a $(\alpha h\nu)^2$ value at slightly higher energy. To make it generalizable we suggest normalizing using a value taken at 2% higher energy than the Tauc gap that has been determined by the fitting process, ie. @ $h\nu = 1.02E_g$. To generalize this further and make the concept applicable to indirect materials, also, we take the square root and correct for the 2% difference in photon

energy to arrive at a factor we call the "Near-Edge Absorptivity Ratio", or NEAR, which is essentially the ratio of the absorption coefficients at those two energy values.

$$NEAR = 1.02\left\{\frac{(\alpha h\nu)^2|_{h\nu=E_{gap}}}{(\alpha h\nu)^2|_{h\nu=1.02E_{gap}}}\right\}^{1/2} = \frac{\alpha(E_{gap})}{\alpha(1.02E_{gap})} \qquad (2)$$

Note that this ratio is dimensionless and can thus be evaluated from $(\alpha\ h\ \nu)^2$ graphs even when arbitrary units are used in the plots. The +2% offset is arbitrary and merely intended to probe how steep the curve is close to the Tauc gap. Similarly, when the NEAR factor would be applied to an indirect-gap material (where the $(\alpha\ h\ \nu)^n$ would have been plotted with a ½ power, then the ratio would need to be squared to yield a dimensionless absorption coefficient ratio.

We have evaluated this ratio for all of the redigitized Tauc plots and provide some analysis of its utility in the next section.

Results

Following the fitting protocol described above, we have digitized and re-fit over 120 Tauc plots on nominally-pure ZnO thin film materials. This has allowed a statistical evaluation of the Tauc method as well as giving us the ability to calculate the NEAR values for all of these samples.[4]

---------- Supplemental material inserted here for review ----------

[4] See supplementary material as [***URL will be inserted according to publisher***] for specific quantities, including NEAR values from each of the subject graphs from the literature along with the original source's Tauc gap value and our refitting of the Tauc gap.

Table 1. Compilation and analysis of example literature where Tauc analyses have been conducted on ZnO thin films.

Reported Tauc Gap (eV)	Re-fitted Tauc Gap (eV)	Near-Edge Absorptivity Ratio	Citation
3.372	3.38	0.42	Abraham[49]
3.387	3.39	0.40	Abraham[49]
3.456	3.46	0.53	Abraham[49]
3.530	3.53	0.45	Abraham[49]
3.625	3.63	0.39	Abraham[49]
3.19	3.20	0.63	Bandyopadhyay[50]
3.22	3.21	0.41	Bandyopadhyay[50]
3.24	3.24	0.58	Bandyopadhyay[50]
3.28	3.30	0.67	Baviskar[51]
3.28	3.24	0.79	Baviskar[104]
3.2	3.13	0.91	Baviskar[104]
3.22	3.17	0.63	Baviskar[104]
3.25	3.23	0.75	Baviskar[104]
3.41	3.39	0.56	Biswas[9]
3.29	3.29	0.53	Bojorge[105]
3.291	3.29	0.41	Caglar[53]
3.288	3.29	0.40	Caglar[53]
3.284	3.29	0.45	Caglar[53]
3.295	3.30	0.37	Caglar[53]
3.211	3.35	0.94	Chawla[55]
3.27	3.27	0.57	Chen[56]
3.26	3.26	0.36	Craciun[58]
3.22	3.25	0.81	Dimitriev[60]
3.27	3.25	0.69	Dimitriev[60]
3.25	3.27	0.70	Dimitriev[60]
3.27	3.29	0.70	Dimitriev[60]
3.45	3.45	0.94	Faraj[61]
3.42	3.47	0.95	Faraj[61]
3.375	3.49	0.93	Faraj[61]
3.28	3.27	0.62	Ghodsi[102]
3.3	3.30	0.32	Gulino[106]
3.3	3.25	0.77	Gurav[62]
3.27	3.28	0.51	Hammouda[63]
3.204	3.11	0.98	Hantehzadeh[64]
3.179	3.16	0.92	Hantehzadeh[64]
3.238	3.17	0.91	Hantehzadeh[64]
3.41	3.41	0.52	He[34]
3.47	3.48	0.58	He[34]
3.24	3.24	0.66	Ho[65]
3.26	3.24	0.67	Ho[65]
3.24	3.25	0.57	Ho[65]
3.24	3.23	0.74	Hong[66]
3.2	3.19	0.78	Hong[66]

3.16	3.17	0.84	Hong[66]
3.14	3.16	0.88	Hong[66]
3.12	3.17	0.90	Hong[66]
3.42	3.42	0.61	Hsu[67]
3.36	3.36	0.65	Hsu[67]
3.32	3.33	0.63	Hsu[67]
3.24	3.25	0.75	Kumar[32]
3.21	3.25	0.82	Kumar
3.29	3.31	0.56	Kumar
3.32	3.34	0.66	Kumar
3.248	3.28	0.52	Liu[107]
3.253	3.25	0.63	Liu
3.261	3.26	0.53	Liu
3.02	3.17	0.82	Lu[108]
3.19	3.26	0.96	Lu
3.36	3.33	0.59	Ma[109]
3.38	3.34	0.61	Ma
3.39	3.36	0.54	Ma
3.268	3.26	0.48	Malek[28]
3.280	3.26	0.41	Malek
3.266	3.27	0.44	Malek
3.281	3.28	0.42	Malek
3.275	3.28	0.59	Malek
3.24	3.25	0.55	Mandal[110]
3.28	3.28	0.58	Mandal
3.3	3.31	0.59	Mandal
3.32	3.32	0.61	Mandal
3.18	3.17	0.39	Marotti[111]
3.21	3.17	0.27	Marotti
3.26	3.25	0.35	Marotti
3.28	3.28	0.60	Millon[68]
3.14	3.14	0.44	Mishra[70]
3.16	3.16	0.69	Mohamed[112]
3.17	3.17	0.83	Mouet[113]
3.19	3.18	0.70	Nehru[75]
3.24	3.23	0.53	Ozutok[114]
3.26	3.25	0.43	Ozutok
3.27	3.27	0.45	Ozutok
3.25	3.23	0.53	Ozutok
3.11	3.14	0.82	Panda[115]
3.24	3.22	0.77	Panda
3.2	3.23	0.66	Panda
3.24	3.26	0.85	Panda
3.41	3.41	0.44	Ramirez[116]
3.26	3.27	0.42	Raoufi[117]
3.27	3.27	0.43	Raoufi
3.28	3.27	0.48	Raoufi
3.17	3.16	0.82	Rusu[118]
3.19	3.16	0.78	Rusu
3.28	3.28	0.34	Sali[77]
3.12	3.02	0.74	Shinde[79]
3.28	3.27	0.93	Shinde
3.19	3.17	0.62	Smirnov[84]

3.21	3.18	0.62	Smirnov
3.447	3.47	0.75	Tan[87]
3.437	3.49	0.49	Tan
3.406	3.39	0.63	Tan
3.403	3.42	0.57	Tan
3.400	3.43	0.50	Tan
3.350	3.36	0.64	Tan
3.295	3.29	0.58	Tan
3.25	3.23	0.53	Tanskanen[88]
3.29	3.29	0.40	Tari[89]
3.3	3.31	0.56	Tari
3.28	3.28	0.79	Tricot[90]
3.22	3.22	0.63	Tsay[93]
3.26	3.26	0.51	Tsay[92, 93]
3.27	3.27	0.51	Tsay[91, 93]
3.2	3.21	0.61	Tuzemen[119]
3.26	3.26	0.66	Tuzemen
3.31	3.31	0.64	Tuzemen
3.2	3.17	0.57	Tuzemen[94]
3.19	3.18	0.50	Tuzemen
3.21	3.19	0.64	Tuzemen
3.27	3.28	0.49	Wang[47]
3.25	3.24	0.39	Yang[98]
3.343	3.35	0.68	Yang[100]
3.18	3.21	0.65	Yang[101]

---------- End supplemental material ----------

It is recognized that that our analysis brings together an extremely large number of measurements of (ideally) the same composition ZnO material in thin film form, though admittedly examining a wide range of different possible microstructures due to their different processing histories. As a first measure of the population under study we plot the cumulative probability distribution of E_g values as reported in the original publication, as shown in Figure 4. While a general sigmoidal shape is evident, the curve jogs to the right at high energy showing that the entire population cannot be fit with a single gaussian distribution. In fact, if we fit the central part as a normal population it requires a mean at 3.266 eV with a standard deviation of

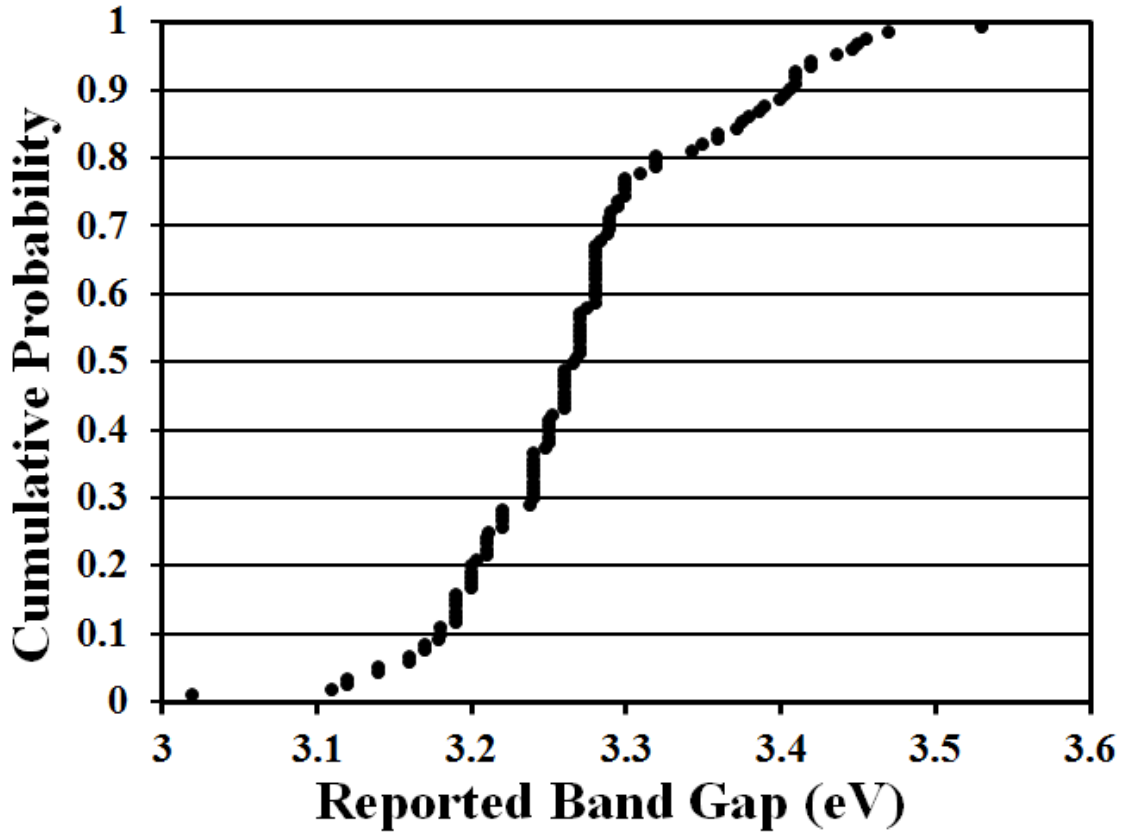

Figure 4: Cumulative probability distribution of literature reported band gap value of zinc oxide determined by the Tauc method (see Table 1 for specific values and source citations).

0.051 eV, but with *two* apparent extra subpopulations, one at higher energies and one at lower. We discuss some possible reasons for these groups in a later section.

Next it is important to evaluate how well the redigitization process has worked for extracting and fitting the band gap from graphical data. Figure 5 displays the cumulative probability distribution of the *difference* between the reported band gap and the value we have obtained with our regression process. The difference data follow a distribution much more

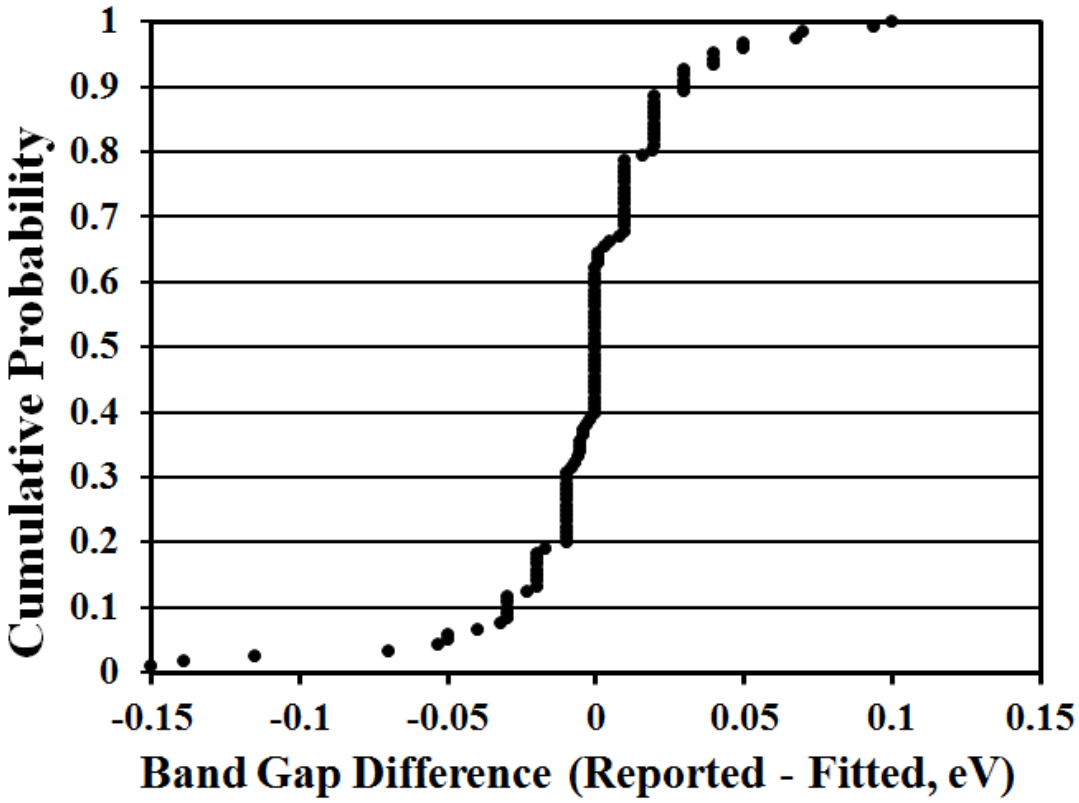

Figure 5: Comparison of bandgap as reported by orginal publication ("Reported") to the assessed bandgap found here with re-digitized data ("Fitted"). The difference between the two is plotted in the format of a cumulative probability distribution over the sample population.

tightly grouped around zero difference between the two populations, with tails extended on the low and high end. The central 60% of the studies have an agreement of +/- 0.01 eV when comparing the reported E_g and our digitized reassessment of the E_g. While there may be many sources of error (see discussion below), the tight distribution shown here substantiates the simple Tauc method and the ease with which data can be digitized from good plots. We take the observed error to represent the relative precision of the method when performed on individual

datasets. The fitting data was compiled from many samples and groups, so it is likely that the comparisons between samples from one researcher would have a higher precision.

Finally, using the digitized curve shapes we have evaluated the Near-Edge Absorptivity Ratio for every plot, as discussed above. Again, to get a measure of the values typically found for ZnO thin film studies (and perhaps representative of values that would be found for other direct-gap thin film materials) we plot a cumulative probability distribution as shown in Figure 6. This curve is reasonably well represented by a normal distribution with mean of 0.60 and a standard deviation of 0.16, though again there is evidence of a small excess subpopulation at higher NEAR values.

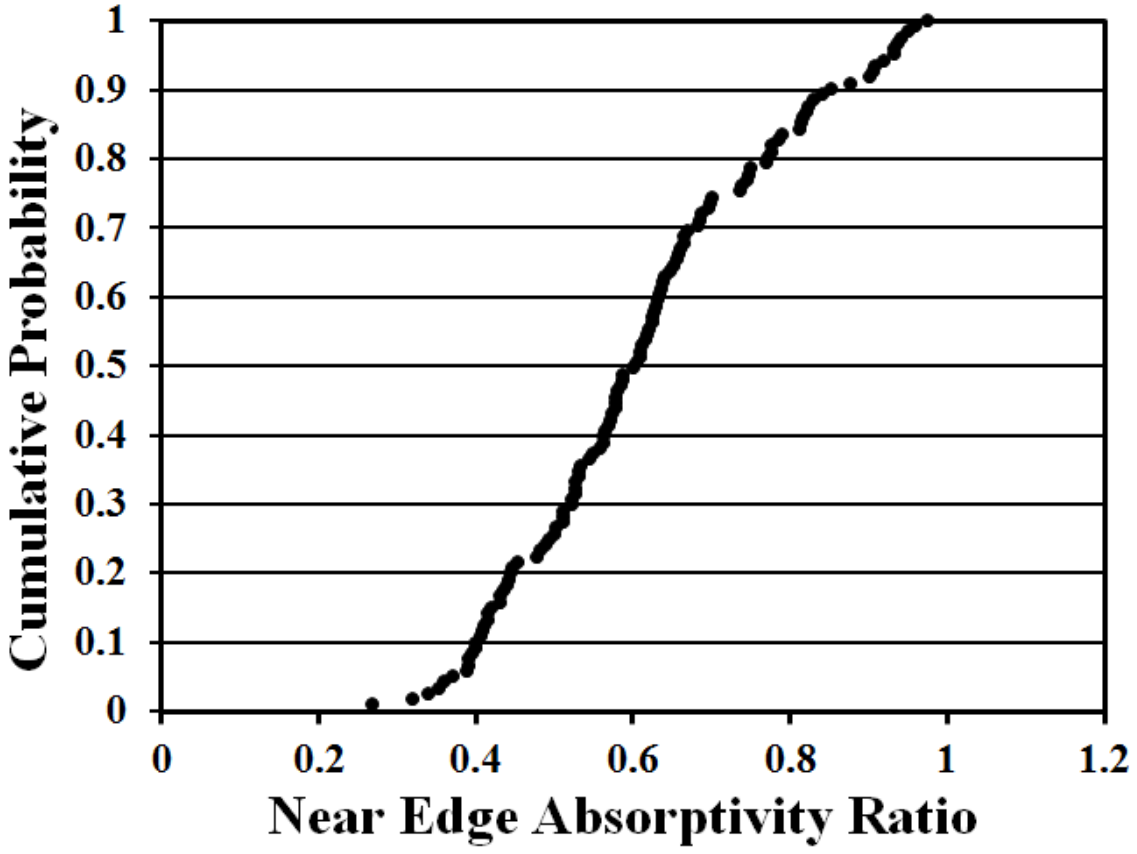

Figure 6: Cumulative probability distribution of the Near-Edge Absorptivity Ratio, as discussed in the text.

Discussion

As shown above, the Tauc method is a reasonable and simple technique for determining a characteristic optical band gap of a thin film material. We've shown that even working from redigitized graphical data, the technique is precise at a level of 0.01 eV, however, the range of values of Tauc gap found in the literature for ZnO films span a very wide range, ~3.1 to ~3.5 eV (see Figure 4), which, of course, significantly stems from materials differences, microstructure development progression, and possible stress-optical or quantum confinement effects. Before digging in to these and other possibilities, we first examine the correlation between the Tauc gap values that are determined and the shape of the Tauc plot, as represented by the NEAR factor. Recalling that the master plot of Tauc gap values (Figure 4) seemed to have extra frequencies at both low and high gap value, we subdivide the population into three groupings with low, medium and high Tauc gap values – taking them in 30%, 40%, and 30% quantities, respectively. Figure 7 gives the cumulative probability distribution for the NEAR factor for each of these subpopulations. It is interesting to see that the "Low" group, with ●'s, is significantly shifted to the right compared to the "Medium" and "High" groups. This is likely caused by samples that have more intense Urbach tailing or sub-gap absorption and are therefore more likely to undergo Tauc plot fitting that includes some of this tail intensity – forcing the Tauc gap intercept to be somewhat lower than would be expected for the ideal material. Given that the "Medium" and "High" distributions are so similar, then we suggest that extra population distribution found before at high Tauc gap values (see Figure 4) must be rooted in physical differences in those samples when compared with thin layers of ideal single crystal material. In one further analysis step, we use the NEAR factor as a guide, suggesting that smaller NEAR values will indicate coatings or thin films that have higher inherent crystallinity (and lower Urbach tailing, as a

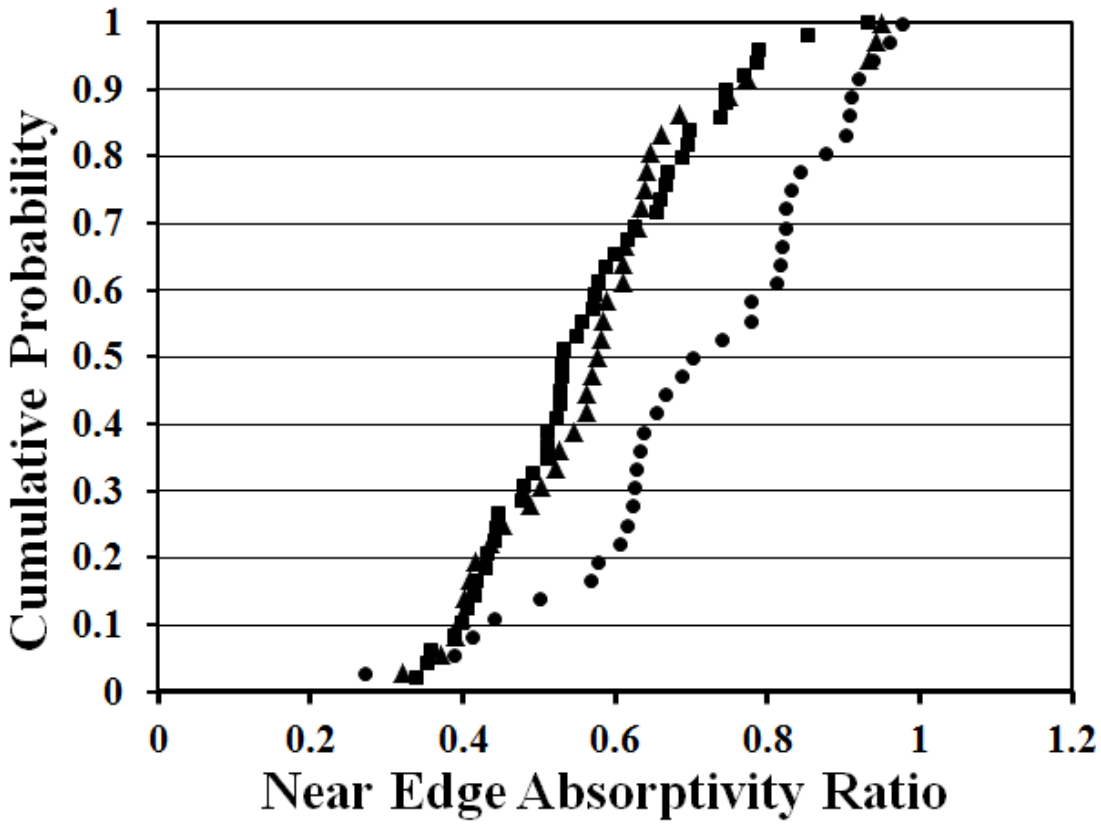

Figure 7: Cumulative probability distribution of the Near-Edge Absorptivity Ratio for subpopulations grouped according to their reported Tauc gap as discussed in the text (c.f. Figure 4): (●) subpopulation with lowest 30% of reported E_g values, (■) subpopulation with middle 40% of reported E_g values, and (▲) subpopulation with highest 30% of reported E_g values.

result). Figure 8 illustrates this concept by comparing the Tauc gap values derived only from samples with the relatively smaller NEAR values (taking the lowest 50% of the whole population). Immediately, two things are evident: (1) the main part of the distribution is significantly tighter than found for the whole population, and (2) the High-gap fraction seems to have been retained and perhaps enhanced. Observation 1 suggests that the NEAR factor is smaller for samples that are more similar to each other – and by inference might be more representative of good intrinsic ZnO material. For example, we can fit this sub-distribution very

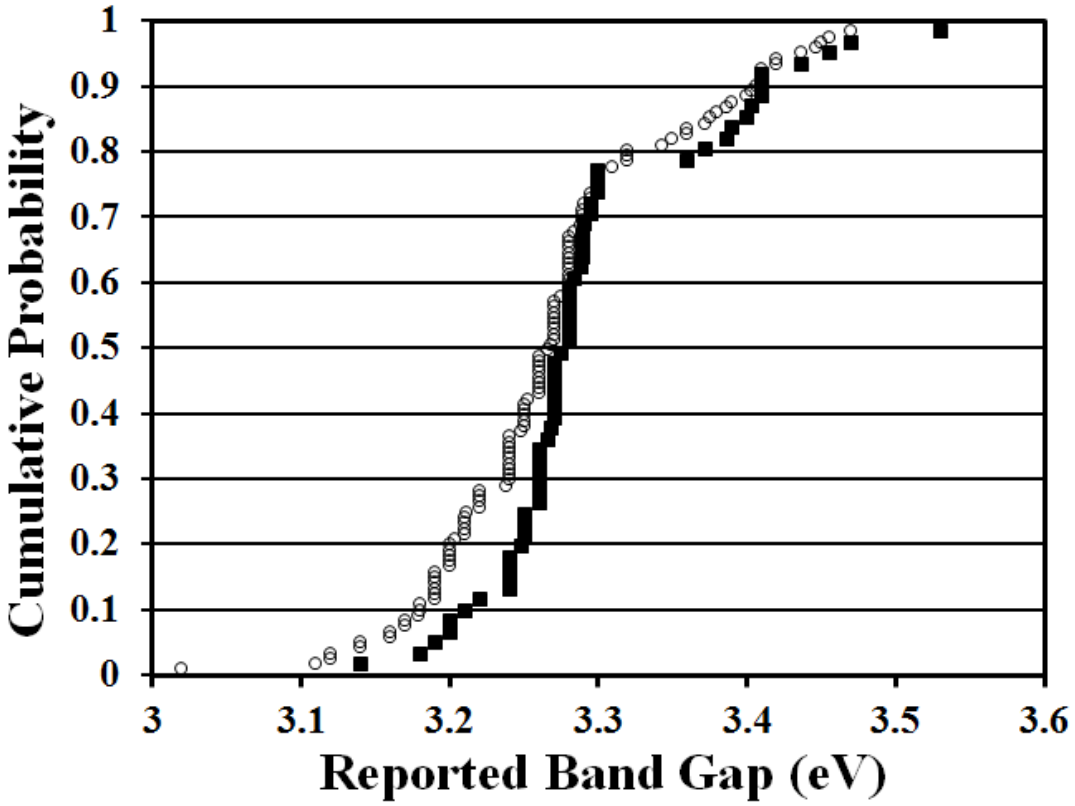

Figure 8: Cumulative probability distribution of the Tauc gap for the subpopulation having the Near-Edge Absorptivity Ratio among the lower half of the whole population. Open circles show the full population for comparison.

nicely with an average of 3.276 and a standard deviation of 0.033 eV. Given that this is a population of more than 60 samples and fabricated using many methods in many labs around the world, then this has to be viewed as an amazingly tight distribution! For comparison, Dawson et al[121] reported an accuracy of 0.02 eV when using three different fitting methods on the same set of samples.

We turn our attention now to observation 2 – that there are many data points showing high Tauc gap even though resulting from Tauc plot shapes that have small NEAR factors. One

paper that contributed five of these data points (Abraham and Dekany[49]) came from samples with particle size ranging from 3.2 to 7.1 nm, which exhibited band gap values ranging from 3.625 eV down to 3.372 eV as particles grew with time suggestive of a quantum confinement effect. Bahneman et al. [122] have looked at the optical properties of tiny ZnO particles and also observed a significantly wider gap for particles smaller than about 5nm. Another group (Tan et al. [85]) found a significant blue-shift in their optical data, too. Because of the low processing temperatures for some of their samples they attributed the larger gap values to the material being amorphous rather than crystalline. Finally, two of these data points come from the work of Ma, et al.[109] who attribute the larger effective gap measurements to a Burstein-Moss shift [123] where stronger reduction during deposition makes the sample more n-type and therefore pushes the predominant absorptions to higher photon energy values. Similarly, there are nanoparticle hydrostatic pressure effects that can also be at play[124]. Srikant and Clarke have performed an especially careful calculation of the stress-induced band-edge shifts for thin films subject to thermal expansion differences between the ZnO films and the substrate[125]. They predict a 0.023 eV increase between their C- and R-plane sapphire deposition orientations, which is close to the experimental increase of 0.030 eV that was observed. On the other hand, for their samples deposited on fused-silica the predicted stress-optic shift is in the opposite direction from the experimental finding. However, when deposited on an amorphous substrate the resultant ZnO morphology had a grain size of 30-80 nm and a much more extensive Urbach tail suggesting that grain boundary states were responsible.

These specific cases show that there are quantum confinement and solid-state physics effects that tend to push band gap values up. However, these are not the only effects that might contribute to changes in the perceived optical band gap. For example, if the samples being tested

have minority second phases then the optical properties may be derived, at least partly, from these second phase particles. And, certainly, the possibility of amorphous phase and Urbach-tail mid-gap states is critical as these are already known to contribute to the lower energy part of the absorption spectrum. Finally, it has been suggested that other approximations of the optical absorption physics for disordered materials may be more physically appropriate and scalable to different thicknesses of material (see for example the work of Cody et al.[126, 127], which has been discussed specifically in comparison with the Tauc method by Mok and O'Leary[128]). Still, it might be argued that a direct-gap material with a strong tendency to crystallize (ZnO) might behave much differently from a hydrogen-terminated, dangling-bond-based, disordered material like amorphous silicon.

Clearly, the subpopulation with smaller NEAR values has a much tighter distribution of band gap values determined using the Tauc method. As noted above, these samples give an average band gap value of 3.276 with a standard deviation of 0.033 eV. The Urbach tails are suggested to be responsible for the slightly lower band gap shifts when the NEAR factor is somewhat larger as a result of mathematical curve-fitting limitations. These are not artifacts and are not noise, but do complicate the use of the Tauc analysis. There is a potential for confusion if the near-edge absorption ratio is found to be relatively large (e.g. NEAR > ~0.7, or so). If the ratio is small (e.g. NEAR < 0.5), there exists a greater probability of good Tauc analysis usage and comparisons between different researchers and sample sources.

Conclusions

An assessment of the Tauc analysis method with respect to consistency, accuracy, application to polycrystalline materials and potential risk of underestimation of the bandgap was

undertaken. The reproduction of a broad survey of literature based analyses in a consistent manner found that the method is robustly accurate even when applied by multiple researchers. The precision of the method was established with the finding that among over 120 analyses, the majority of refits were within 0.01 eV of the originally-determined Tauc gap values. Further, when half of the studies are excluded (based on their larger near-edge-absorptivity-ratios), we have demonstrated an accuracy of the technique at the ~0.03 eV level, or about 1% of the absolute value of the band gap, at least under conditions that yield the sharper Tauc plots with smaller near-edge-absorptivity-ratios. This variation includes all manners of unintentional distortion of the bandgap, and so this result is particularly notable. The investigation involved the interrogation of zinc oxide, a typically-stoichiometric pure semiconductor of polycrystalline nature. That the Tauc analyses are accurate and valid for this polycrystalline semiconductor suggests that the analysis technique is applicable to not just the amorphous materials originally examined by Tauc et al[1], but to polycrystalline semiconductors as a class. Finally, the near-edge absorptivity ratio (NEAR) quantification of the degree of disorder imparted by Urbach tails has been introduced and used to guide evaluation of Tauc plot fitting quality.

Acknowledgements

This work was supported in part by National Science Foundation Grant No. 0903661 "IGERT: Nanotechnology for Clean Energy." Further support from the Corning/Saint-Gobain/McLaren Endowment is also greatly appreciated.

References

1. Tauc, J., R. Grigorovici and A. Vancu, *Optical properties and electronic structure of amorphous germanium.* Physica Status Solidi, 1966. **15**: p. 627-637.
2. Ozgur, U., Y.I. Alivov, C. Liu, A. Teke, M.A. Reshchikov, S. Dogan, V. Avrutin, S.J. Cho and H. Morkoc, *A comprehensive review of ZnO materials and devices.* Journal of Applied Physics, 2005. **98**(4).
3. Ozgur, U., D. Hofstetter and H. Morkoc, *ZnO Devices and Applications: A Review of Current Status and Future Prospects.* Proceedings of the Ieee, 2010. **98**(7): p. 1255-1268.
4. Yoshino, Y., M. Takeuchi, K. Inoue, T. Makino, S. Arai and T. Hata, *Control of temperature coefficient of frequency in zinc oxide thin film bulk acoustic wave resonators at various frequency ranges.* Vacuum, 2002. **66**(3-4): p. 467-472.
5. Gupta, T.K., *APPLICATION OF ZINC-OXIDE VARISTORS.* Journal of the American Ceramic Society, 1990. **73**(7): p. 1817-1840.
6. Rodnyi, P.A. and I.V. Khodyuk, *Optical and luminescence properties of zinc oxide (Review).* Optics and Spectroscopy, 2011. **111**(5): p. 776-785.
7. Huang, M.H., S. Mao, H. Feick, H.Q. Yan, Y.Y. Wu, H. Kind, E. Weber, R. Russo and P.D. Yang, *Room-temperature ultraviolet nanowire nanolasers.* Science, 2001. **292**(5523): p. 1897-1899.
8. Bagnall, D.M., Y.F. Chen, Z. Zhu, T. Yao, S. Koyama, M.Y. Shen and T. Goto, *Optically pumped lasing of ZnO at room temperature.* Applied Physics Letters, 1997. **70**(17): p. 2230-2232.
9. Biswas, P., S. Kundu, P. Banerji and S. Bhunia, *Super rapid response of humidity sensor based on MOCVD grown ZnO nanotips array.* Sensors and Actuators B-Chemical, 2013. **178**: p. 331-338.
10. Mitra, P., A.P. Chatterjee and H.S. Maiti, *Chemical deposition of ZnO films for gas sensors.* Journal of Materials Science-Materials in Electronics, 1998. **9**(6): p. 441-445.
11. Mitra, P., A.P. Chatterjee and H.S. Maiti, *ZnO thin film sensor.* Materials Letters, 1998. **35**(1-2): p. 33-38.
12. Rao, B.B., *Zinc oxide ceramic semi-conductor gas sensor for ethanol vapour.* Materials Chemistry and Physics, 2000. **64**(1): p. 62-65.
13. Kumar, B.R. and T.S. Rao, *Influence of Sputtering Power on Physical Properties of Nanostructured Zinc Aluminum Oxide Thin Films For Photovoltaic Applications.* Digest Journal of Nanomaterials and Biostructures, 2012. **7**(3): p. 1051-1061.
14. Platzer-Bjorkman, C., T. Torndahl, D. Abou-Ras, J. Malmstrom, J. Kessler and L. Stolt, *Zn(O,S) buffer layers by atomic layer deposition in Cu(In,Ga)Se-2 based thin film solar cells: Band alignment and sulfur gradient.* Journal of Applied Physics, 2006. **100**(4).
15. Jiang, M.L., K. Tang and X.Z. Yan, *Characterization of intrinsic ZnO thin film deposited by sputtering and its effects on CuIn1-xGaxSe2 solar cells.* Journal of Photonics for Energy, 2012. **2**.
16. Lin, Y.C., T.Y. Chen, L.C. Wang and S.Y. Lien, *Comparison of AZO, GZO, and AGZO Thin Films TCOs Applied for a-Si Solar Cells.* Journal of the Electrochemical Society, 2012. **159**(6): p. H599-H604.
17. Abb, M., B. Sepulveda, H.M.H. Chong and O.L. Muskens, *Transparent conducting oxides for active hybrid metamaterial devices.* Journal of Optics, 2012. **14**(11).
18. Kim, W.H., W.J. Maeng, M.K. Kim and H. Kim, *Low Pressure Chemical Vapor Deposition of Aluminum-Doped Zinc Oxide for Transparent Conducting Electrodes.* Journal of the Electrochemical Society, 2011. **158**(8): p. D495-D499.
19. Wilken, S., D. Scheunemann, V. Wilkens, J. Parisi and H. Borchert, *Improvement of ITO-free inverted polymer-based solar cells by using, colloidal zinc oxide nanocrystals as electron-selective buffer layer.* Organic Electronics, 2012. **13**(11): p. 2386-2394.

20. Yoshino, Y., T. Makino, Y. Katayama and T. Hata, *Optimization of zinc oxide thin film for surface acoustic wave filters by radio frequency sputtering.* Vacuum, 2000. **59**(2-3): p. 538-545.
21. Thomas, D.G., *The exciton spectrum of zinc oxide.* Journal of Physics and Chemistry of Solids, 1960. **15**(1-2): p. 86-96.
22. Srikant, V. and D.R. Clarke, *On the optical band gap of zinc oxide.* Journal of Applied Physics, 1998. **83**(10): p. 5447-5451.
23. Jellison, G.E. and L.A. Boatner, *Optical functions of uniaxial ZnO determined by generalized ellipsometry.* Physical Review B, 1998. **58**(7): p. 3586-3589.
24. Aksoy, S., Y. Caglar, S. Ilican and M. Caglar, *Sol-gel derived Li-Mg co-doped ZnO films: Preparation and characterization via XRD, XPS, FESEM.* Journal of Alloys and Compounds, 2012. **512**(1): p. 171-178.
25. Su, B.Y., S.Y. Chu, Y.D. Juang, M.C. Lin, C.C. Chang and C.J. Wu, *Efficiency Enhancement of GaAs Photovoltaics Due to Sol-Gel Derived Anti-Reflective AZO Films.* Journal of the Electrochemical Society, 2012. **159**(3): p. H312-H316.
26. Yang, S.H. and Y.L. Zhang, *Structural, optical and magnetic properties of Mn-doped ZnO thin films prepared by sol-gel method.* Journal of Magnetism and Magnetic Materials, 2013. **334**: p. 52-58.
27. Talebian, N., M.R. Nilforoushan and N. Maleki, *Ultraviolet to visible-light range photocatalytic activity of ZnO films prepared using sol-gel method: The influence of solvent.* Thin Solid Films, 2013. **527**: p. 50-58.
28. Malek, M.F., M.H. Mamat, M.Z. Sahdan, M.M. Zahidi, Z. Khusaimi and M.R. Mahmood, *Influence of various sol concentrations on stress/strain and properties of ZnO thin films synthesised by sol-gel technique.* Thin Solid Films, 2013. **527**: p. 102-109.
29. Tsay, C.Y. and W.C. Lee, *Effect of dopants on the structural, optical and electrical properties of sol-gel derived ZnO semiconductor thin films.* Current Applied Physics, 2013. **13**(1): p. 60-65.
30. Zhang, W.Y., D.K. He, Z.Z. Liu, L.J. Sun and Z.X. Fu, *Preparation of transparent conducting Al-doped ZnO thin films by single source chemical vapor deposition.* Optoelectronics and Advanced Materials-Rapid Communications, 2010. **4**(11): p. 1651-1654.
31. Takenaka, K., Y. Okumura and Y. Setsuhara, *Plasma-Assisted Mist Chemical Vapor Deposition of Zinc Oxide Films Using Solution of Zinc Acetate.* Japanese Journal of Applied Physics, 2013. **52**(1).
32. Kumar, S. and P.D. Sahare, *Observation of band gap and surface defects of ZnO nanoparticles synthesized via hydrothermal route at different reaction temperature.* Optics Communications, 2012. **285**(24): p. 5210-5216.
33. Chand, P., A. Gaur and A. Kumar, *Structural and optical properties of ZnO nanoparticles synthesized at different pH values.* Journal of Alloys and Compounds, 2012. **539**: p. 174-178.
34. He, R.L. and T. Tsuzuki, *Low-Temperature Solvothermal Synthesis of ZnO Quantum Dots.* Journal of the American Ceramic Society, 2010. **93**(8): p. 2281-2285.
35. Jager, S., B. Szyszka, J. Szczyrbowski and G. Brauer, *Comparison of transparent conductive oxide thin films prepared by a.c. and d.c. reactive magnetron sputtering.* Surface & Coatings Technology, 1998. **98**(1-3): p. 1304-1314.
36. Kumar, B.R. and T.S. Rao, *Investigations on opto-electronical properties of DC reactive magnetron sputtered zinc aluminum oxide thin films annealed at different temperatures.* Applied Surface Science, 2013. **265**: p. 169-175.
37. Wang, Y., H.L. Wang, Y. Wang, W.Y. Ding, S. Peng and W.P. Chai, *Preparation and properties of surface textured ZnO: Al films by direct current pulse magnetron sputtering.* Journal of Materials Science-Materials in Electronics, 2013. **24**(1): p. 53-57.
38. Elmas, S. and S. Korkmaz, *Deposition of Al doped ZnO thin films on the different substrates with radio frequency magnetron sputtering.* Journal of Non-Crystalline Solids, 2013. **359**: p. 69-72.

39. Wei, X.Q., J.Z. Huang, M.Y. Zhang, Y. Du and B.Y. Man, *Effects of substrate parameters on structure and optical properties of ZnO thin films fabricated by pulsed laser deposition.* Materials Science and Engineering B-Advanced Functional Solid-State Materials, 2010. **166**(2): p. 141-146.
40. Bruncko, J., A. Vincze, M. Netrvalova, P. Sutta, D. Hasko and M. Michalka, *Annealing and recrystallization of amorphous ZnO thin films deposited under cryogenic conditions by pulsed laser deposition.* Thin Solid Films, 2011. **520**(2): p. 866-870.
41. Clatot, J., G. Campet, A. Zeinert, C. Labrugere and A. Rougier, *Room temperature transparent conducting oxides based on zinc oxide thin films.* Applied Surface Science, 2011. **257**(12): p. 5181-5184.
42. Franklin, J.B., B. Zou, P. Petrov, D.W. McComb, M.P. Ryan and M.A. McLachlan, *Optimised pulsed laser deposition of ZnO thin films on transparent conducting substrates.* Journal of Materials Chemistry, 2011. **21**(22): p. 8178-8182.
43. Kisi, E.H. and M.M. Elcombe, *Upsilon-Parameters for the Wurtzite Structure Of ZnS And ZnO Using Powder Neutron-Diffraction.* Acta Crystallographica Section C-Crystal Structure Communications, 1989. **45**: p. 1867-1870.
44. Allsopp, H.J. and J.P. Roberts, *Non-stoichiometry of zinc oxide and its relation to sintering: Part 1 - Determination of non-stoichiometry in zinc oxide.* Transactions of the Faraday Society, 1959: p. 1386.
45. Davis, E.A. and N.F. Mott, *Conduction in non-crystalline systems V. Conductivity, optical absorption and photoconductivity in amorphous semiconductors.* Philosophical Magazine, 1970. **22**: p. 903.
46. Mott, N.F. and E.A. Davis, *Electronic processes in non-crystalline materials*. 2nd ed. 1979: Clarendon Press (Oxford and New York).
47. Wang, M.D., D.Y. Zhu, Y. Liu, L. Zhang, C.X. Zheng, Z.H. He, D.H. Chen and L.S. Wen, *Determination of thickness and optical constants of ZnO thin films prepared by filtered cathode vacuum arc deposition.* Chinese Physics Letters, 2008. **25**(2): p. 743-746.
48. Urbach, F., *The Long-Wavelength Edge of Photographic Sensitivity and of the Electronic Absorption of Solids.* Physical Review 1953. **92**: p. 1324.
49. Abraham, N. and I. Dekany, *Size-dependent photoluminescence properties of bare ZnO and polyethylene imine stabilized ZnO nanoparticles and their Langmuir-Blodgett films.* Colloids and Surfaces a-Physicochemical and Engineering Aspects, 2010. **364**(1-3): p. 26-33.
50. Bandyopadhyay, S., G.K. Paul and S.K. Sen, *Study of optical properties of some sol-gel derived films of ZnO.* Solar Energy Materials and Solar Cells, 2002. **71**(1): p. 103-113.
51. Baviskar, P.K., W.W. Tan, J.B. Zhang and B.R. Sankapal, *Wet chemical synthesis of ZnO thin films and sensitization to light with N3 dye for solar cell application.* Journal of Physics D-Applied Physics, 2009. **42**(12).
52. Bojorge, C.D., H.R. Canepa, U.E. Gilabert, D. Silva, E.A. Dalchiele and R.E. Marotti, *Synthesis and optical characterization of ZnO and ZnO : Al nanocrystalline films obtained by the sol-gel dip-coating process.* Journal of Materials Science-Materials in Electronics, 2007. **18**(11): p. 1119-1125.
53. Caglar, M., S. Ilican, Y. Caglar and F. Yakuphanoglu, *The effects of Al doping on the optical constants of ZnO thin films prepared by spray pyrolysis method.* Journal of Materials Science-Materials in Electronics, 2008. **19**(8-9): p. 704-708.
54. Caglar, M., S. Ilican, Y. Caglar and F. Yakuphanoglu, *Electrical conductivity and optical properties of ZnO nanostructured thin film.* Applied Surface Science, 2009. **255**(8): p. 4491-4496.
55. Chawla, A.K., D. Kaur and R. Chandra, *Structural and optical characterization of ZnO nanocrystalline films deposited by sputtering.* Optical Materials, 2007. **29**(8): p. 995-998.

56. Chen, J.J., H. Deng, N. Li, Y.L. Tian and H. Ji, *Realization of nonpolar a-plane ZnO films on r-plane sapphire substrates using a simple single-source chemical vapor deposition.* Materials Letters, 2011. **65**(4): p. 716-718.
57. Choi, S.Y., M.J. Kang, T.J. Park, R. Tap, S. Schoemaker and M. Willert-Porada, *Electrical and optical properties of ZnO films deposited by ECR-PECVD.* Physica Status Solidi a-Applications and Materials Science, 2006. **203**(10): p. R73-R75.
58. Craciun, V., J. Elders, J.G.E. Gardeniers and I.W. Boyd, *CHARACTERISTICS OF HIGH-QUALITY ZNO THIN-FILMS DEPOSITED BY PULSED-LASER DEPOSITION.* Applied Physics Letters, 1994. **65**(23): p. 2963-2965.
59. Craciun, V., D. Craciun, M.C. Bunescu, R. Dabu and I.W. Boyd, *Growth of highly transparent oxide layers by pulsed laser deposition: Reduction of droplet density.* Applied Surface Science, 1997. **109**: p. 354-358.
60. Dimitriev, Y., M. Gancheva and R. Iordanova, *Effects of the mechanical activation of zinc carbonate hydroxide on the formation and properties of zinc oxides.* Journal of Alloys and Compounds, 2012. **519**: p. 161-166.
61. Faraj, M.G. and K. Ibrahim, *Optical and Structural Properties of Thermally Evaporated Zinc Oxide Thin Films on Polyethylene Terephthalate Substrates.* International Journal of Polymer Science, 2011.
62. Gurav, K.V., V.J. Fulari, U.M. Patil, C.D. Lokhande and O.S. Joo, *Room temperature soft chemical route for nanofibrous wurtzite ZnO thin film synthesis.* Applied Surface Science, 2010. **256**(9): p. 2680-2685.
63. Hammouda, A., A. Canizares, P. Simon, A. Boughalout and M. Kechouane, *Improving the sensitivity of Raman signal of ZnO thin films deposited on silicon substrate.* Vibrational Spectroscopy, 2012. **62**: p. 217-221.
64. Hantehzadeh, M.R., P.S. Dezfooli and S.A. Hoseini, *Effect of O-2/Ar Mixture on the Structural and Optical Properties of ZnO Thin Films Fabricated by DC Cylindrical Magnetron Sputtering.* Journal of Fusion Energy, 2012. **31**(3): p. 298-303.
65. Ho, Y.S. and K.Y. Lee, *Fabrication of highly oriented (002) ZnO film on glass by sol-gel method.* Thin Solid Films, 2010. **519**(4): p. 1431-1434.
66. Hong, R.J., J.D. Shao, H.B. He and Z.X. Fan, *Influence of buffer layer thickness on the structure and optical properties of ZnO thin films.* Applied Surface Science, 2006. **252**(8): p. 2888-2893.
67. Hsu, J.C., Y.H. Lin, P.W. Wang and Y.Y. Chen, *Spectroscopic ellipsometry studies on various zinc oxide films deposited by ion beam sputtering at room temperature.* Applied Optics, 2012. **51**(9): p. 1209-1215.
68. Millon, E., O. Albert, J.C. Loulergue, J. Etchepare, D. Hulin, W. Seiler and J. Perriere, *Growth of heteroepitaxial ZnO thin films by femtosecond pulsed-laser deposition.* Journal of Applied Physics, 2000. **88**(11): p. 6937-6939.
69. Mir, N., M. Salavati-Niasari and F. Davar, *Preparation of ZnO nanoflowers and Zn glycerolate nanoplates using inorganic precursors via a convenient rout and application in dye sensitized solar cells.* Chemical Engineering Journal, 2012. **181**: p. 779-789.
70. Mishra, D.K., P. Kumar, M.K. Sharma, J. Das, S.K. Singh, B.K. Roul, S. Varma, R. Chatterjee, V.V. Srinivasu and D. Kanjilal, *Ferromagnetism in ZnO single crystal.* Physica B-Condensed Matter, 2010. **405**(12): p. 2659-2663.
71. Nagaraja, K.K., S. Pramodini, P. Poornesh and H.S. Nagaraja, *Effect of annealing on the structural and nonlinear optical properties of ZnO thin films under cw regime.* Journal of Physics D-Applied Physics, 2013. **46**(5).

72. Dhananjay, J. Nagaraju and S.B. Krupanidh, *Investigations on multimagnetron sputtered Zn(1-x)Mg(x)O thin films through metal-ferroelectric-semiconductor configuration.* Journal of Applied Physics, 2008. **104**(4).
73. Natsume, Y. and H. Sakata, *Zinc oxide films prepared by sol-gel spin-coating.* Thin Solid Films, 2000. **372**(1-2): p. 30-36.
74. Natsume, Y. and H. Sakata, *Electrical conductivity and optical properties of ZnO films annealed in hydrogen atmosphere after chemical vapor deposition.* Journal of Materials Science-Materials in Electronics, 2001. **12**(2): p. 87-92.
75. Nehru, L.C., V. Swaminathan and C. Sanjeeviraja, *Rapid synthesis of nanocrystalline ZnO by a microwave-assisted combustion method.* Powder Technology, 2012. **226**: p. 29-33.
76. Ng, Z.N., K.Y. Chan and T. Tohsophon, *Effects of annealing temperature on ZnO and AZO films prepared by sol-gel technique.* Applied Surface Science, 2012. **258**(24): p. 9604-9609.
77. Sali, S., M. Boumaour, M. Kechouane, S. Kermadi and F. Aitamar, *Nanocrystalline ZnO film deposited by ultrasonic spray on textured silicon substrate as an anti-reflection coating layer.* Physica B-Condensed Matter, 2012. **407**(13): p. 2626-2631.
78. Sharma, P.K., A.C. Pandey, G. Zolnierkiewicz, N. Guskos and C. Rudowicz, *Relationship between oxygen defects and the photoluminescence property of ZnO nanoparticles: A spectroscopic view.* Journal of Applied Physics, 2009. **106**(9).
79. Shinde, V.R., T.P. Gujar and C.D. Lokhande, *Studies on growth of ZnO thin films by a novel chemical method.* Solar Energy Materials and Solar Cells, 2007. **91**(12): p. 1055-1061.
80. Singh, P., A.K. Chawla, D. Kaur and R. Chandra, *Effect of oxygen partial pressure on the structural and optical properties of sputter deposited ZnO nanocrystalline thin films.* Materials Letters, 2007. **61**(10): p. 2050-2053.
81. Singh, P., A. Kumar, Deepak and D. Kaur, *Growth and characterization of ZnO nanocrystalline thin films and nanopowder via low-cost ultrasonic spray pyrolysis.* Journal of Crystal Growth, 2007. **306**(2): p. 303-310.
82. Singh, P., A. Kumar, Deepak and D. Kaur, *ZnO nanocrystalline powder synthesized by ultrasonic mist-chemical vapour deposition.* Optical Materials, 2008. **30**(8): p. 1316-1322.
83. Singh, P., A. Kumar, A. Kaushal, D. Kaur, A. Pandey and R.N. Goyal, *In situ high temperature XRD studies of ZnO nanopowder prepared via cost effective ultrasonic mist chemical vapour deposition.* Bulletin of Materials Science, 2008. **31**(3): p. 573-577.
84. Smirnov, M., C. Baban and G.I. Rusu, *Structural and optical characteristics of spin-coated ZnO thin films.* Applied Surface Science, 2010. **256**(8): p. 2405-2408.
85. Tan, S.T., B.J. Chen, X.W. Sun, W.J. Fan, H.S. Kwok, X.H. Zhang and S.J. Chua, *Blueshift of optical band gap in ZnO thin films grown by metal-organic chemical-vapor deposition.* Journal of Applied Physics, 2005. **98**(1).
86. Tan, S.T., B.J. Chen, X.W. Sun, M.B. Yu, X.H. Zhang and S.J. Chua, *Realization of-intrinsic p-type ZnO thin films by metal organic chemical vapor deposition.* Journal of Electronic Materials, 2005. **34**(8): p. 1172-1176.
87. Tan, S.T., B.J. Chen, X.W. Sun, X. Hu, X.H. Zhang and S.J. Chua, *Properties of polycrystalline ZnO thin films by metal organic chemical vapor deposition.* Journal of Crystal Growth, 2005. **281**(2-4): p. 571-576.
88. Tanskanen, J.T., J.R. Bakke, T.A. Pakkanen and S.F. Bent, *Influence of organozinc ligand design on growth and material properties of ZnS and ZnO deposited by atomic layer deposition.* Journal of Vacuum Science & Technology A, 2011. **29**(3).
89. Tari, O., A. Aronne, M.L. Addonizio, S. Daliento, E. Fanelli and P. Pernice, *Sol-gel synthesis of ZnO transparent and conductive films: A critical approach.* Solar Energy Materials and Solar Cells, 2012. **105**: p. 179-186.

90. Tricot, S., M. Nistor, E. Millon, C. Boulmer-Leborgne, N.B. Mandache, J. Perriere and W. Seiler, *Epitaxial ZnO thin films grown by pulsed electron beam deposition.* Surface Science, 2010. **604**(21-22): p. 2024-2030.
91. Tsay, C.Y., K.S. Fan, C.Y. Chen, J.M. Wu and C.M. Lei, *Effect of preheating process on crystallization and optical properties of sol-gel derived ZnO semiconductor thin films.* Journal of Electroceramics, 2011. **26**(1-4): p. 23-27.
92. Tsay, C.Y., K.S. Fan, S.H. Chen and C.H. Tsai, *Preparation and characterization of ZnO transparent semiconductor thin films by sol-gel method.* Journal of Alloys and Compounds, 2010. **495**(1): p. 126-130.
93. Tsay, C.Y., K.S. Fan, Y.W. Wang, C.J. Chang, Y.K. Tseng and C.K. Lin, *Transparent semiconductor zinc oxide thin films deposited on glass substrates by sol-gel process.* Ceramics International, 2010. **36**(6): p. 1791-1795.
94. Tuzemen, E.S., S. Eker, H. Kavak and R. Esen, *Dependence of film thickness on the structural and optical properties of ZnO thin films.* Applied Surface Science, 2009. **255**(12): p. 6195-6200.
95. Wang, T., Y.M. Liu, Q.Q. Fang, M.Z. Wu, X. Sun and F. Lu, *Low temperature synthesis wide optical band gap Al and (Al, Na) co-doped ZnO thin films.* Applied Surface Science, 2011. **257**(6): p. 2341-2345.
96. Wang, Y.G., S.P. Lau, H.W. Lee, S.F. Yu, B.K. Tay, X.H. Zhang, K.Y. Tse and H.H. Hng, *Comprehensive study of ZnO films prepared by filtered cathodic vacuum arc at room temperature.* Journal of Applied Physics, 2003. **94**(3): p. 1597-1604.
97. Xia, J.A., X.H. Lu, C.S. Wang, Y.X. Tong and L.P. Chen, *Electrochemical Assemble of Single Crystalline Twin ZnO Nanorods.* Journal of the Electrochemical Society, 2011. **158**(5): p. D244-D247.
98. Yang, C., X.M. Li, Y.F. Gu, W.D. Yu, X.D. Gao and Y.W. Zhang, *ZnO based oxide system with continuous bandgap modulation from 3.7 to 4.9 eV.* Applied Physics Letters, 2008. **93**(11).
99. Yang, L., P.W. May, L. Yin and T.B. Scott, *Growth of self-assembled ZnO nanoleaf from aqueous solution by pulsed laser ablation.* Nanotechnology, 2007. **18**(21).
100. Yang, S.H., Y. Liu, Y.L. Zhang and D. Mo, *Investigation of annealing-treatment on structural and optical properties of sol-gel-derived zinc oxide thin films.* Bulletin of Materials Science, 2010. **33**(3): p. 209-214.
101. Yang, W.Y., Q. Li, S.A. Gao and J.K. Shang, *NH4+ directed assembly of zinc oxide micro-tubes from nanoflakes.* Nanoscale Research Letters, 2011. **6**.
102. Ghodsi, F.E. and H. Absalan, *Comparative Study of ZnO Thin Films Prepared by Different Sol-Gel Route.* Acta Physica Polonica A, 2010. **118**(4): p. 659-664.
103. Tsay, C.Y., M.C. Wang and S.C. Chiang, *Characterization of Zn1-x Mg (x) O Films Prepared by the Sol-Gel Process and Their Application for Thin-Film Transistors.* Journal of Electronic Materials, 2009. **38**(9): p. 1962-1968.
104. Baviskar, P.K., P.R. Nikam, S.S. Gargote, A. Ennaoui and B.R. Sankapal, *Controlled synthesis of ZnO nanostructures with assorted morphologies via simple solution chemistry.* Journal of Alloys and Compounds, 2013. **551**: p. 233-242.
105. Bojorge, C.D., V.R. Kent, E. Teliz, H.R. Canepa, R. Henriquez, H. Gomez, R.E. Marotti and E.A. Dalchiele, *Zinc-oxide nanowires electrochemically grown onto sol-gel spin-coated seed layers.* Physica Status Solidi a-Applications and Materials Science, 2011. **208**(7): p. 1662-1669.
106. Gulino, A., F. Lupo and M.E. Fragala, *Substrate-free, self-standing ZnO thin films.* Journal of Physical Chemistry C, 2008. **112**(36): p. 13869-13872.
107. Liu, K.C., Y.H. Lu, Y.H. Liao and B.S. Huang, *Utilizing transparent ZnO thin film as permeation barrier to improve light outcoupling and longevity of top-emission polymer light-emitting devices.* Japanese Journal of Applied Physics, 2008. **47**(4): p. 3162-3166.

108. Lu, X.H., D. Wang, G.R. Li, C.Y. Su, D.B. Kuang and Y.X. Tong, *Controllable Electrochemical Synthesis of Hierarchical ZnO Nanostructures on FTO Glass.* Journal of Physical Chemistry C, 2009. **113**(31): p. 13574-13582.
109. Ma, X.L., J. Zhang, J.G. Lu and Z.Z. Ye, *Room temperature growth and properties of ZnO films by pulsed laser deposition.* Applied Surface Science, 2010. **257**(4): p. 1310-1313.
110. Mandal, S., R.K. Singha, A. Dhar and S.K. Ray, *Optical and structural characteristics of ZnO thin films grown by rf magnetron sputtering.* Materials Research Bulletin, 2008. **43**(2): p. 244-250.
111. Marotti, R.E., J.A. Badan, E. Quagliata and E.A. Dalchiele, *Red photoluminescence and band edge shift from ZnO thin films.* Physica B-Condensed Matter, 2007. **398**(2): p. 337-340.
112. Mohamed, S.H., H.M. Ali, H.A. Mohamed and A.M. Salem, *Effect of annealing and In content on the properties of electron beam evaporated ZnO films.* European Physical Journal-Applied Physics, 2005. **31**(2): p. 95-99.
113. Mouet, T., T. Devers, A. Telia, Z. Messai, V. Harel, K. Konstantinov, I. Kante and M.T. Ta, *Growth and characterization of thin ZnO films deposited on glass substrates by electrodeposition technique.* Applied Surface Science, 2010. **256**(13): p. 4114-4120.
114. Ozutok, F., B. Demirselcuk, E. Sarica, S. Turkyilmaz and V. Bilgin, *Study of Ultrasonically Sprayed ZnO Films: Thermal Annealing Effect.* Acta Physica Polonica A, 2012. **121**(1): p. 53-55.
115. Panda, S.K. and C. Jacob, *Preparation of transparent ZnO thin films and their application in UV sensor devices.* Solid-State Electronics, 2012. **73**: p. 44-50.
116. Ramirez, D., D. Silva, H. Gomez, G. Riveros, R.E. Marotti and E.A. Dalchiele, *Electrodeposition of ZnO thin films by using molecular oxygen and hydrogen peroxide as oxygen precursors: Structural and optical properties.* Solar Energy Materials and Solar Cells, 2007. **91**(15-16): p. 1458-1461.
117. Raoufi, D. and T. Raoufi, *The effect of heat treatment on the physical properties of sol-gel derived ZnO thin films.* Applied Surface Science, 2009. **255**(11): p. 5812-5817.
118. Rusu, D.I., G.G. Rusu and D. Luca, *Structural Characteristics and Optical Properties of Thermally Oxidized Zinc Films.* Acta Physica Polonica A, 2011. **119**(6): p. 850-856.
119. Tuzemen, E.S., H. Kavak and R. Esen, *Influence of oxygen pressure of ZnO/glass substrate produced by pulsed filtered cathodic vacuum arc deposition.* Physica B-Condensed Matter, 2007. **390**(1-2): p. 366-372.
120. Sweenor, D.E., S.K. O'Leary and B.E. Foutz, *On defining the optical gap of an amorphous semiconductor: an empirical calibration for the case of hydrogenated amorphous silicon.* Solid State Communications, 1999. **110**(5): p. 281-286.
121. Dawson, R.M., Y.M. Li, M. Gunes, D. Heller, S. Nag, R.W. Collins, C.R. Wronski and M. Bennett. *Optical Properties of Hydrogenated Amorphous Silicon, Silicon-Germanium, and Silicon-Carbon Thin Films*. in *Materials Research Society Proceedings **258**, 595-600*. 1992.
122. Bahnemann, D.W., C. Kormann and M.R. Hoffmann, *Preparation and Characterization of Quantum Size Zinc-Oxide - A Detailed Spectroscopic Study.* Journal of Physical Chemistry, 1987. **91**(14): p. 3789-3798.
123. Lin, J.P. and J.M. Wu, *The effect of annealing processes on electronic properties of sol-gel derived Al-doped ZnO films.* Applied Physics Letters, 2008. **92**(13).
124. Mang, A., K. Reimann and S. Rubenacke, *Band-Gaps, Crystal-Field Splitting, Spin-Orbit-Coupling, and Exciton Binding-Energies in ZnO Under Hydrostatic-Pressure.* Solid State Communications, 1995. **94**(4): p. 251-254.
125. Srikant, V. and D.R. Clarke, *Optical absorption edge of ZnO thin films: The effect of substrate.* Journal of Applied Physics, 1997. **81**(9): p. 6357-6364.
126. Cody, G.D., B.G. Brooks and B. Abeles, *Optical absorption above the optical gap of amorphous silicon hydride.* Solar Energy Materials 1982. **8**: p. 231-240.

127. Cody, G.D., *The Optical-Absorption Edge of a-Si-H.* Semiconductors and Semimetals, 1984. **21**: p. 11-82.
128. Mok, T.M. and S.K. O'Leary, *The dependence of the Tauc and Cody optical gaps associated with hydrogenated amorphous silicon on the film thickness: alpha l Experimental limitations and the impact of curvature in the Tauc and Cody plots.* Journal of Applied Physics, 2007. **102**(11).